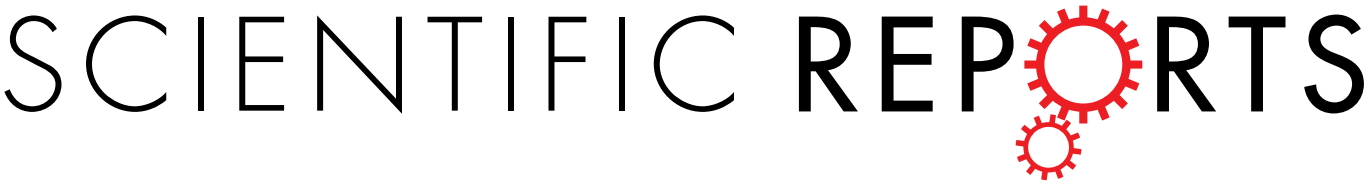

OPEN

Simulated effect of calcification feedback on atmospheric CO_2 and ocean acidification

Received: 20 August 2015
Accepted: 30 December 2015
Published: 03 February 2016

Han Zhang[1] & Long Cao[1,2]

Ocean uptake of anthropogenic CO_2 reduces pH and saturation state of calcium carbonate materials of seawater, which could reduce the calcification rate of some marine organisms, triggering a negative feedback on the growth of atmospheric CO_2. We quantify the effect of this CO_2-calcification feedback by conducting a series of Earth system model simulations that incorporate different parameterization schemes describing the dependence of calcification rate on saturation state of $CaCO_3$. In a scenario with SRES A2 CO_2 emission until 2100 and zero emission afterwards, by year 3500, in the simulation without CO_2-calcification feedback, model projects an accumulated ocean CO_2 uptake of 1462 PgC, atmospheric CO_2 of 612 ppm, and surface pH of 7.9. Inclusion of CO_2-calcification feedback increases ocean CO_2 uptake by 9 to 285 PgC, reduces atmospheric CO_2 by 4 to 70 ppm, and mitigates the reduction in surface pH by 0.003 to 0.06, depending on the form of parameterization scheme used. It is also found that the effect of CO_2-calcification feedback on ocean carbon uptake is comparable and could be much larger than the effect from CO_2-induced warming. Our results highlight the potentially important role CO_2-calcification feedback plays in ocean carbon cycle and projections of future atmospheric CO_2 concentrations.

Atmospheric CO_2 concentration has increased by 40% since the preindustrial time[1] primarily due to human activities of fossil fuel burning and deforestation. Between 1959 and 2011 total anthropogenic CO_2 emission is 436 PgC (1PgC = 10^{15} gram carbon = 1 billion ton carbon) with 44% of the emission stayed in the atmosphere, while 29% and 27% of emissions were absorbed by the terrestrial biosphere and the ocean, respectively[2]. Increasing atmospheric CO_2 warms the Earth by trapping long wave radiation. In addition, the oceanic uptake of anthropogenic CO_2 perturbs ocean chemistry by making the ocean more acidic, a process known as ocean acidification[3].

Global warming and ocean acidification would influence many processes of the marine carbon cycle, which in turn affect atmospheric CO_2 and climate change. For instance, rising atmospheric CO_2 concentration leads to an increase of sea surface temperature, reducing CO_2 solubility in the ocean. As a result, a warmer ocean reduces the oceanic CO_2 uptake, which provides a positive feedback to the growth of atmospheric CO_2[4,5]. A warmer ocean could also accelerate respiration/remineralization rate of organic carbon and cause a reduction in the vertical flux of particulate organic carbon (POC) to the abyssal ocean. This reduced vertical transport of POC would weaken the ocean biological pump and decrease the ocean's ability to take up carbon, providing a positive feedback to the growth of atmospheric CO_2[6]. On the other hand, increased C:N:P stoichiometry in seawater due to rising partial pressure of CO_2 in the ocean could enhance extracellular organic matter production, strengthening the ocean biological carbon pump and providing a negative feedback to rising atmospheric CO_2[7–9].

In addition to global warming, ocean acidification, through its effect on the ocean carbon cycle, could provide feedbacks to atmospheric CO_2. Global mean ocean surface pH, which can be used to quantify the degree of ocean acidification, has dropped by 0.1 units[1], representing a 26% increase in hydrogen ion concentration since the industrial revolution. The rise of hydrogen ion concentration would consequently lower carbonate ion concentration ($[CO_3^{2-}]$) and in turn causes a reduction of seawater $CaCO_3$ (aragonite or calcite) saturation state, which is defined as

$$\Omega = [Ca^{2+}][CO_3^{2-}]/K^*_{sp} \quad (1)$$

[1]School of Earth Sciences, Zhejiang University, Hangzhou, Zhejiang 310027, China. [2]State Key Laboratory of Satellite Ocean Environment Dynamics, Second Institute of Oceanography, Hangzhou, Zhejiang, China. Correspondence and requests for materials should be addressed to L.C. (email: longcao@zju.edu.cn)

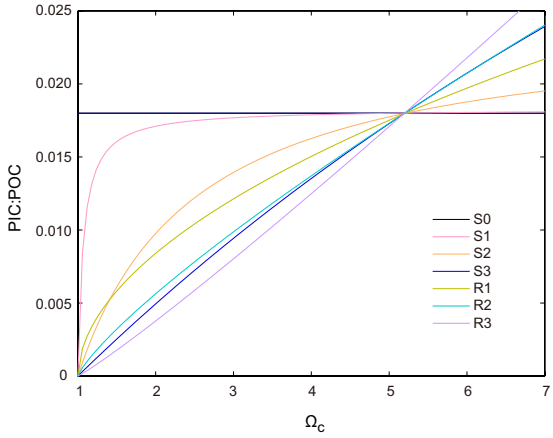

Figure 1. Dependence of $CaCO_3$: POC production ratio ($R^{CaCO_3/POC}$) on Ω_C ($CaCO_3$ saturation state) used in model parameterizations. Detailed configuration of different model versions is provided in Table 1.

Here, K^*_{sp} is the stoichiometric solubility product for aragonite or calcite, which are two different polymorphs of $CaCO_3$[10].

Calcifying organisms that use $CaCO_3$ to precipitate their shells or skeletons may not be able to acclimate to the reduction of $CaCO_3$ saturation state[11]. Gattuso *et al.* detected a nonlinear relationship between calcification rate and $CaCO_3$ saturation state from experimental results of certain types of coral species, and suggested calcification rate may drop substantially as a result of decreasing aragonite saturation state[12]. Langdon *et al.* through mesocosm experiment results, argued that declining aragonite saturation state is a primary factor that attenuates coral reef calcification[11]. Laboratory experiments with coccolithophorids[13,14] and analyses of foraminiferal shell weight observational record across glacial-interglacial Termination[15] indicated a reduction in $CaCO_3$ production with increasing CO_2 concentration and resulting ocean acidification. More recent observational or experiment results also provided evidences of the negative response of calcification to ocean acidification[16–18]. In spite of the abundant observational and experimental evidence, the sensitivity of the response of calcification to acidification varies dramatically between experiments using different species of calcifying groups or manipulation methods.

The process of calcification decreases $[CO_3^{2-}]$, suppressing the ocean's ability to absorb atmospheric CO_2. Therefore, the potential reduction of calcification as a result of CO_2-induced ocean acidification could enhance the ocean's uptake of carbon, providing a negative feedback for rising atmospheric CO_2[19], which is termed as CO_2-calcification feedback here. Recently, a few modeling studies have been conducted to examine effects of the CO_2-calcification feedback. In these studies, the parameterization schemes that link $CaCO_3$ production to $CaCO_3$ saturation state (Ω) are based on different results of experimental studies, and as a consequence, estimates of the effect on oceanic uptake of atmospheric CO_2 from CO_2-calcification feedback varies among studies[20–24].

As an extension of previous studies, here we further examine the effect of CO_2-calcification feedback on the oceanic uptake of atmospheric CO_2. We incorporate the calcification-Ω dependence into an Earth system model of intermediate complexity to quantify the strength of the CO_2-calcification feedback in mitigating the growth of atmospheric CO_2 and ocean acidification. Usually, previous studies on CO_2-calcification feedback assume a single type of calcification-Ω parameterization scheme. Here, different types of calcification-Ω parameterization schemes are used, which enables us to assess the importance in the parameter value (parameter uncertainty) and the equation form (model structural uncertainty) of the calcification response to ocean acidification. Also, we compare the strength of CO_2-calcification feedback with the feedback induced by climate change. Furthermore, we assess the effect of different parameterization of CO_2-calcification feedback on projected ocean acidification. This study aims to further our understanding in the role of the CO_2-calcification feedback on the ocean carbon cycle and atmospheric CO_2, which is important for a reliable projection of future atmospheric CO_2 concentrations and climate change.

Results

To quantify the effect of CO_2-calcification feedback, we conduct a series of Earth system model simulations that incorporate different parameterization schemes representing the dependence of calcification rate on saturation state of $CaCO_3$ (refer to Method section and Fig. 1). All model simulations last from year 1800 to 3500 with SRES A2 CO_2 emission scenario until year 2100 and zero CO_2 emission afterwards. Total cumulative anthropogenic CO_2 emissions amount to 2270 PgC.

To quantify the effect of climate change on the carbon cycle, we also conduct additional simulation experiments in which CO_2-induced warming does not affect the carbon cycle. A detailed description of the model and simulation experiments can be found in the Method section.

Model-observation comparison. To test the performance of the UVic model in simulating present day carbon cycle, the model-simulated distributions of key variables of the ocean carbon cycle are compared with GLODAP observations[25]. As shown in Fig. 2, the simulated vertical profiles of alkalinity and dissolved inorganic

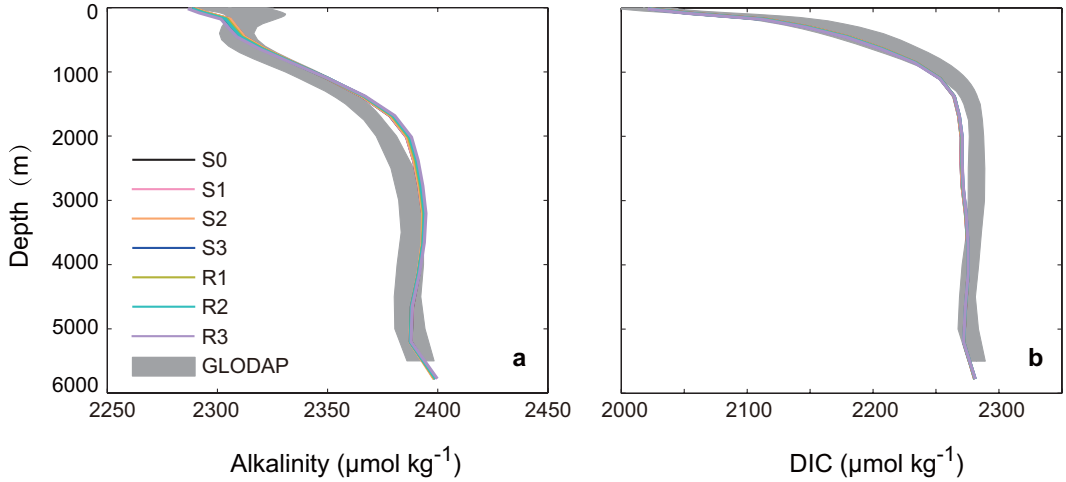

Figure 2. Model-simulated global mean vertical distribution of dissolved inorganic carbon (DIC) and alkalinity (ALK) in mid 1990s compared with observed GLODAP data (including published errors as gray shaded areas)[25]. Model results are shown for different parameterization schemes of CO_2-calcification feedbacks. Detailed configuration of different model versions is provided in Table 1.

carbon (DIC) are in close agreement with observational estimates, and their vertical profiles of different model versions are almost indistinguishable. This is because in different model parameterizations, $R_{max}^{CaCO_3/POC}$ in equation (3) and $R_0^{CaCO_3/POC}$ in equation (4) was back-calculated to ensure that the global mean value of $R^{CaCO_3/POC}$ at preindustrial time is the same for all model versions.

In the simulations with climate change modeled $CaCO_3$ productions with different parameterizations of $R^{CaCO_3/POC}$ in year 2000 range from 0.69–0.73 PgC yr^{-1}, which are within the estimate range of 0.6–1.6 PgC yr^{-1} calculated from observations of satellite and sediment trap[20].

Future projections. In the following, we first present results from simulations including the effect of CO_2-induced warming on the ocean carbon cycle. Then we compare the effect of CO_2-calcification feedback with that from CO_2-induced warming, which is obtained by the differences between the simulations with and without CO_2-induced warming.

As shown in Fig. 3, in the control simulation (S0), by year 2100, the global ocean has absorbed 581 PgC of anthropogenic CO_2. After the cessation of CO_2 emission at 2100, the ocean continues to absorb CO_2, and by year 3500, the global ocean has a total CO_2 uptake of 1462 PgC (Fig. 3b, also see Supplementary Table S1). As for the carbon uptake by the terrestrial biosphere, by year 2100 and 3500 the land has absorbed 629 and 2236 Pg C, respectively (Fig. 3d). Atmospheric CO_2 reaches a peak value of 897 ppm at year 2100 (Fig. 3e). A cessation of CO_2 emission leads to a gradual decline of atmospheric CO_2. By year 3500, atmospheric CO_2 concentration is 612 ppm with a global mean surface warming of 3.9 °C (Fig. 3f). The ocean's absorption of anthropogenic CO_2 acidifies the global ocean (Fig. 4). By year 2100, relative to the preindustrial values, surface mean pH drops by 0.42 units, corresponding to a 50.6% reduction in surface $[CO_3^{2-}]$. With the gradual decrease of atmospheric CO_2, surface ocean acidification slowly recovers. By year 3500, surface mean pH reduces by 0.29 units, corresponding to a 37.8% decrease of $[CO_3^{2-}]$ relative to the preindustrial values (see Supplementary Table S1 online).

The introduction of $R^{CaCO_3/POC}$ dependence on calcite saturation state (Ω_C) affects the ocean carbon cycle through its impact on the production of $CaCO_3$. In the S0 simulation, $CaCO_3$ production increases with time (Fig. 5) mainly as a result of increasing ocean temperature that boosts the growth of phytoplankton, which $CaCO_3$ production depends on according to equation (2). In the simulations with Ω_C-dependent $R^{CaCO_3/POC}$, $CaCO_3$ productions are under the influence of both changing temperature and Ω_C. As shown in Fig. 5, except for S1, relative to the preindustrial value, there is a general decrease of $CaCO_3$ production with time, indicating the dominant influence of decreasing Ω_C. After around year 2150, there appears to be a recovery of $CaCO_3$ production as a result of the recovery of surface $[CO_3^{2-}]$ (Fig. 5). In the simulation of S2, after year 2350, the change of $CaCO_3$ production becomes positive again, indicating the increasing influence of rising ocean temperature. Overall, compared to the simulation of S0, the introduction of Ω_C-dependent $R^{CaCO_3/POC}$ greatly decreases the production of $CaCO_3$, which has great implication for the oceanic uptake of CO_2 as discussed below.

The change in $CaCO_3$ production has great impact on the ocean alkalinity. In the simulation of S0, an increase in $CaCO_3$ production (Fig. 5) leads to a decrease in ocean-mean alkalinity (Fig. 4). In the simulations with the Ω_C-dependent $R^{CaCO_3/POC}$, ocean-mean alkalinity generally increases with time. For example, in the simulation of R3, by year 3500, ocean-mean and surface-mean alkalinity have increased by 25 and 24 μmol kg^{-1} respectively (see Supplementary Table S1 online). Meanwhile, in the simulations that include the Ω_C-dependent $R^{CaCO_3/POC}$, the vertical gradient of alkalinity diminishes due to the reduced $CaCO_3$ production rate and the consequent weaker $CaCO_3$ pump (Fig. 6, see Supplementary Fig. S1 online).

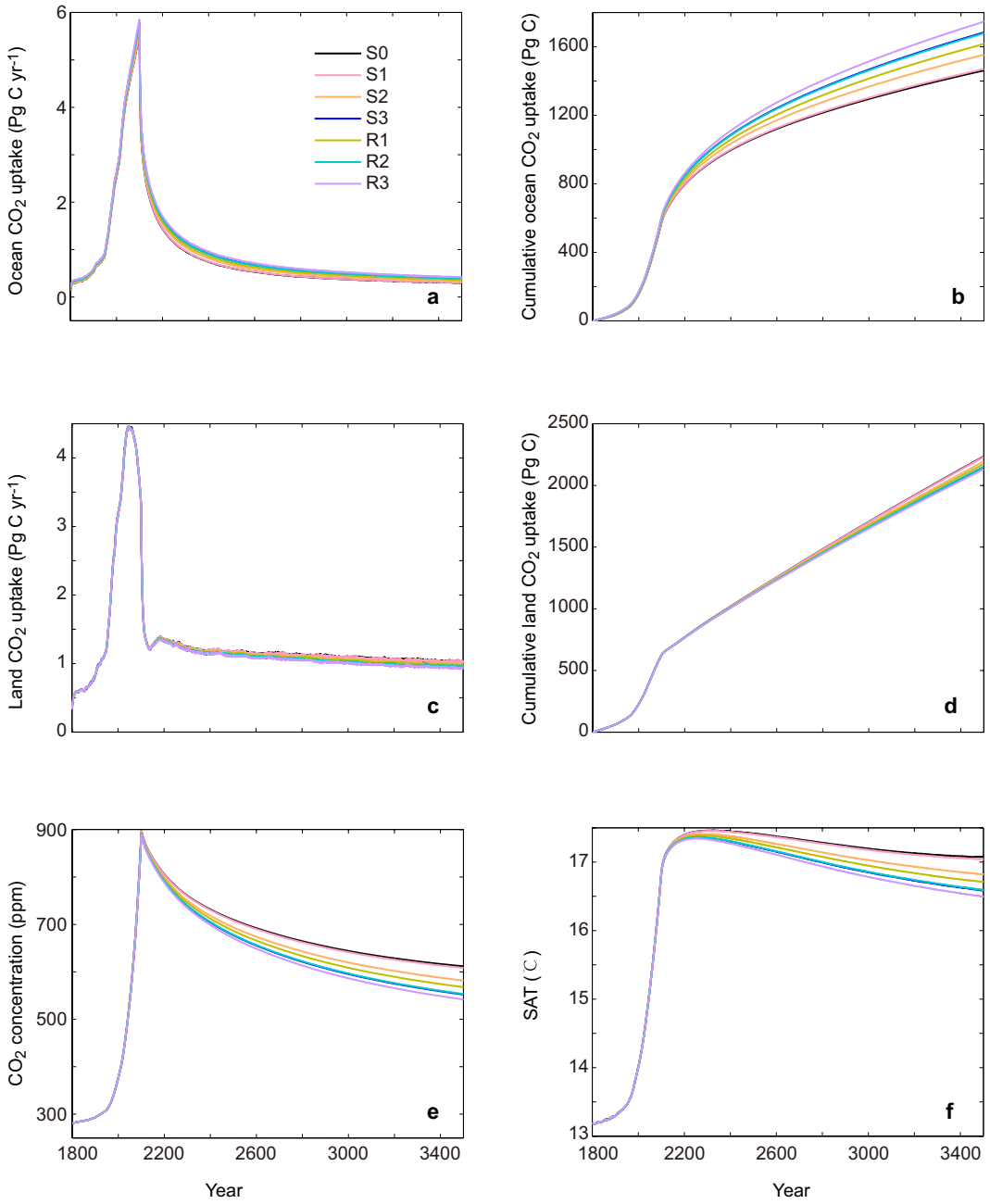

Figure 3. Model-simulated time series of annual and global mean variables for (a) ocean CO_2 uptake, (b) cumulative ocean CO_2 uptake, (c) land CO_2 uptake, (d) cumulative land CO_2 uptake (e) atmospheric CO_2 concentration, (f) surface air temperature (SAT). Model results are shown for different parameterization schemes of CO_2-calcification feedbacks. Detailed configuration of different model versions is provided in Table 1.

As a result of modification of the ocean alkalinity, the Ω_C-dependent $R^{CaCO_3/POC}$ affects the ocean's uptake of CO_2. By year 2100, compared to the S0 simulation, the inclusion of Ω_C-dependent $R^{CaCO_3/POC}$ increases accumulated oceanic CO_2 uptake by 1 PgC (0.1%) to 36 PgC (6.2%), depending on the exact form of $CaCO_3$ production parameterization (Fig. 3). By year 3500, the increase in accumulated oceanic CO_2 uptake relative to the simulation of S0 ranges from 9 PgC (0.6%) to 285 PgC (19.5%) across different $CaCO_3$ production parameterization schemes (Fig. 3, see Supplementary Table S1 online). As a consequence, by year 3500, simulated atmospheric CO_2 ranges from 608 to 542 ppm with the inclusion of dependence of $R^{CaCO_3/POC}$ on Ω_C, compared with 612 ppm in the S0 simulation (Fig. 3). Moreover, by year 3500, the inclusion of Ω_C-dependent $R^{CaCO_3/POC}$ acts to reduce the amount of surface warming by 0.04 to 0.6 K relative to the S0 simulation, depending on the $R^{CaCO_3/POC}$ parameterization scheme used (see Supplementary Table S1 online).

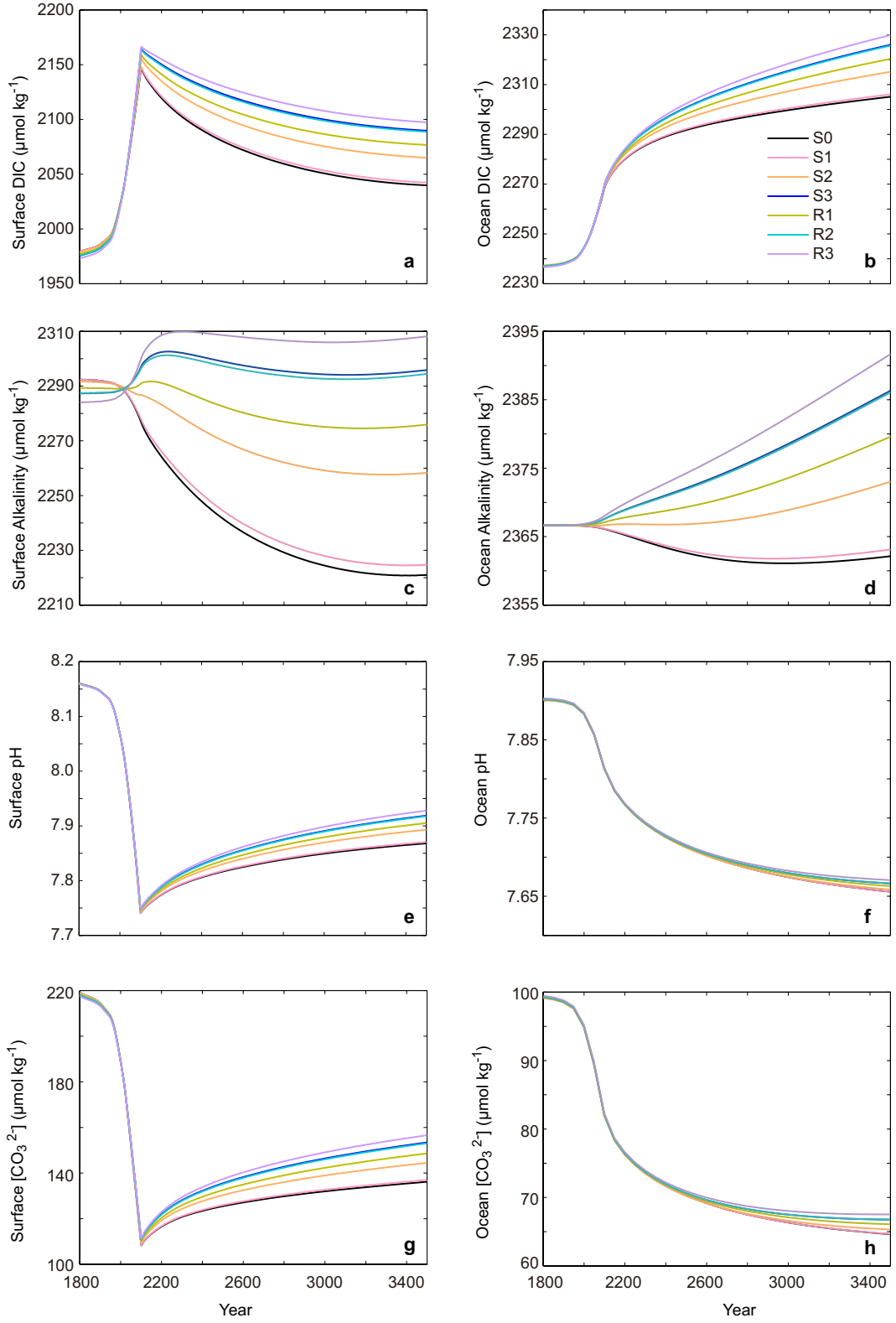

Figure 4. Model-simulated time series of global mean variables as a function of year for (a) ocean surface dissolved inorganic carbon (DIC) concentration, (b) ocean mean DIC concentration, (c) ocean surface alkalinity concentration, (d) ocean mean alkalinity concentration, (e) ocean surface pH, (f) ocean mean pH, (g) ocean surface $[CO_3^{2-}]$, (h) ocean mean $[CO_3^{2-}]$. Detailed configuration of different model versions is provided in Table 1.

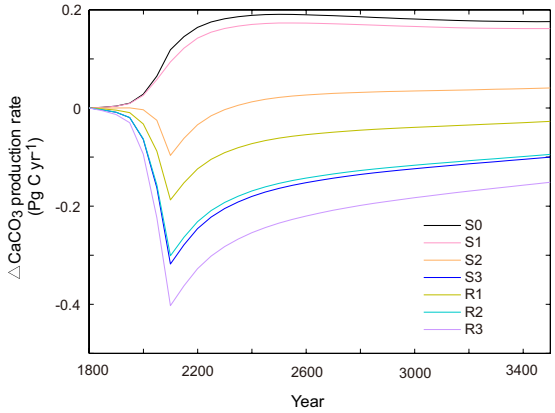

Figure 5. Model-simulated time series of annual and global mean change in $CaCO_3$ production rate for different parameterization schemes of CO_2-calcification feedbacks. Detailed configuration of different model versions is provided in Table 1.

The inclusion of $R^{CaCO_3/POC}$ dependence on Ω_C also has a great influence on ocean acidification (Fig. 4 e, f, g, h). For example, by year 3500, the difference of surface mean pH between R3 and S0 becomes 0.06 units, corresponding to a 15% difference of $[CO_3^{2-}]$ (see Supplementary Table S1 online). Thus, the inclusion of Ω_C-dependent $R^{CaCO_3/POC}$ increases the ocean uptake of CO_2, but mitigates ocean acidification. The mitigation of ocean acidification in the simulations with $R^{CaCO_3/POC}$ dependence of Ω_C, relative to the simulation with fixed $R^{CaCO_3/POC}$ is mainly a result of increased alkalinity, which dominates the effect of increased DIC on ocean acidification.

In the above, we have discussed model-simulated results with the inclusion of CO_2-induced warming. To test the importance of CO_2-induced warming on the ocean carbon cycle, we have performed additional simulations that do not include the radiative effect of increasing atmospheric CO_2. Our simulations show that, by year 3500, in the S0 case, in the absence of CO_2-induced warming effect, model-simulated cumulative ocean's uptake of CO_2 is 122 PgC greater than that in the simulation with CO_2-induced warming (Fig. 7, see Supplementary Fig. S2, Supplementary Table S1 online). For comparison, relative to the S0 simulation, by year 3500, the inclusion of Ω_C -dependent $R^{CaCO_3/POC}$ increases the ocean's uptake of CO_2 by 9 to 285 PgC (Fig. 7, see Supplementary Fig. S2, Supplementary Table S1 online). This comparison shows that in terms of the magnitude of oceanic CO_2 uptake, the effect of CO_2-calcification feedback could be comparable to or even much larger than that from the feedback of CO_2-induced warming.

Discussion

Here, we use the UVic model to quantify the effect of potential CO_2-calcification feedback on the projections of the ocean carbon cycle and climate change. To evaluate the effect of CO_2-calcification feedback on the ocean carbon cycle and associated uncertainties, we include two different types of parameterization schemes that link $CaCO_3$ production with saturation state of calcite. In each scheme, a set of different parameters is used. As atmospheric CO_2 increases and the ocean becomes more acidic, the introduction of Ω_C-dependent $R^{CaCO_3/POC}$ decreases the production of $CaCO_3$, increasing ocean alkalinity and enhancing the oceanic uptake of atmospheric CO_2. Therefore, it triggers negative feedbacks on the growth of atmospheric CO_2 and curbs global warming to a certain degree. Under SRES A2 CO_2 emission scenario with zero emission after year 2100 and a total cumulative emission of 2270 PgC, relative to the simulation with fixed $CaCO_3$: POC production ratio, by year 2100, the simulations that include CO_2-calcification feedback decrease modeled atmospheric CO_2 by 0.1 to 7 ppm; by year 3500, the simulations that include CO_2-calcification feedback decrease modeled atmospheric CO_2 concentration by 4 to 70 ppm. The magnitude of the CO_2-calcification feedback depends on the calcification-Ω_C parameterization scheme used and parameter values used, demonstrating the importance of both the model structure uncertainty and parameter uncertainty of the CO_2-calcification feedback in regulating the ocean carbon cycle. While the inclusion of the CO_2-calcification feedback enhances the ocean's uptake of atmospheric CO_2, it acts to mitigate ocean acidification mainly as a result of increased ocean alkalinity. For example, by year 3500, the inclusion of Ω_C -dependent $R^{CaCO_3/POC}$ increases surface mean pH and $[CO_3^{2-}]$ by 0.8% and 15.0% in R3 relative to S0. Furthermore, our simulations show that the effect of CO_2-calcification feedback on ocean's uptake of atmospheric CO_2 is comparable to, and in some cases, much larger than the effect from CO_2-induced warming.

Our study shows a noticeable CO_2-calcification feedback on atmospheric CO_2. Different estimates of this feedback are reported in previous modeling studies[21–24]. For example, Ridgwell *et al.* by using the function form of equation (4) to represent CO_2-calcification feedback, reported that under a CO_2 emission scenario that reaches a total of 4,000 PgC, the inclusion of CO_2-calcification feedback would lower atmospheric CO_2 concentration by 29–93 ppm by year 3000, depending on the parameter values used[21]. Hofmann and Schellnhuber[22], using an exponential form that links calcification rate to carbonate ion concentration, predicted a 125 ppm decrease in atmospheric CO_2 by year 3000 as a result of CO_2-calcification feedback under a scenario with total anthropogenic CO_2 emission of 4,075 PgC. Other studies show relatively small effects from the CO_2-calcification feedback. For instance, Heinze, using a linear relationship that links calcification to seawater CO_2 partial pressure, projected

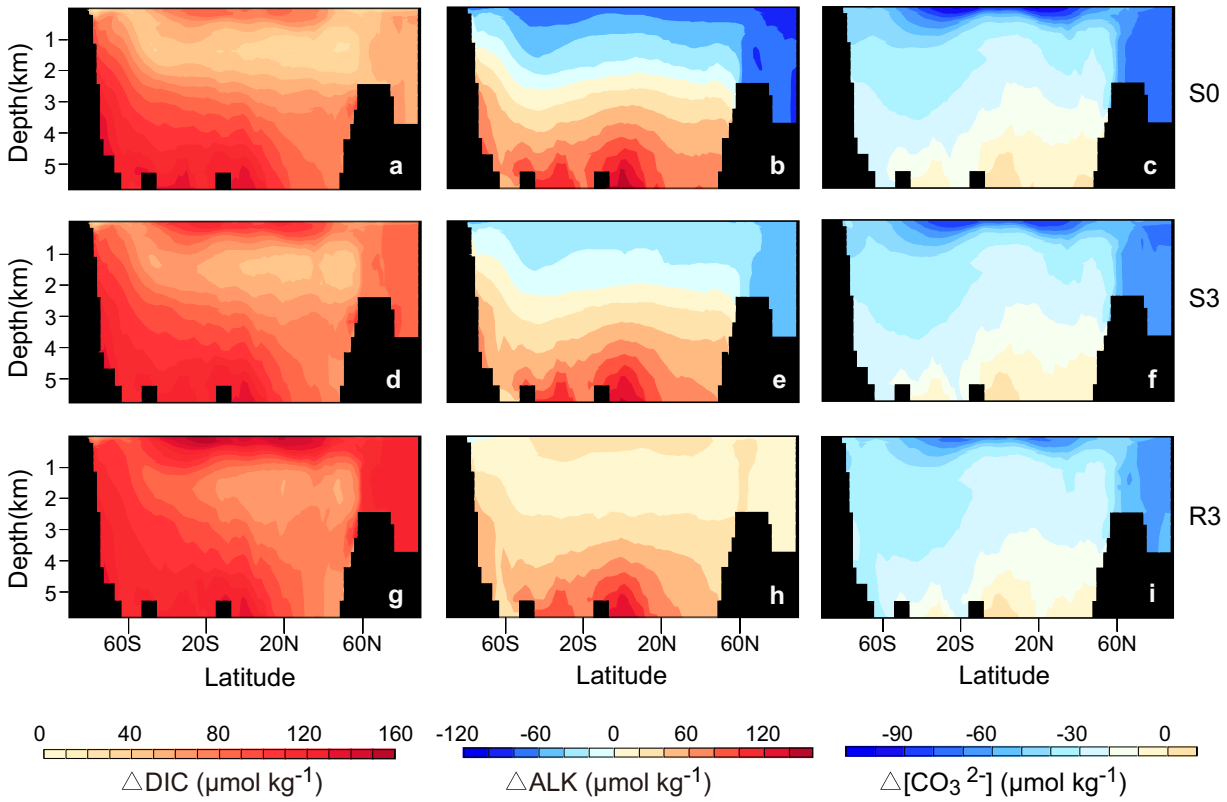

Figure 6. Model-simulated latitude-depth distribution of the change in DIC (year 3500 minus year 1800) ΔDIC (a,d,g), the change in ALK (year 3500 minus year 1800) ΔALK (b,e,h), and the change in $[CO_3^{2-}]$ (year 3500 minus year 1800) $\Delta[CO_3^{2-}]$ (c,f,i). Results are shown for simulation S0 (**a**–**c**), simulation S3 (**d**–**f**), and simulation R3 (**g**–**i**), respectively. Detailed configuration of different model versions is provided in Table 1. The figures were generated using UV-CDAT (http://uvcdat.llnl.gov/).

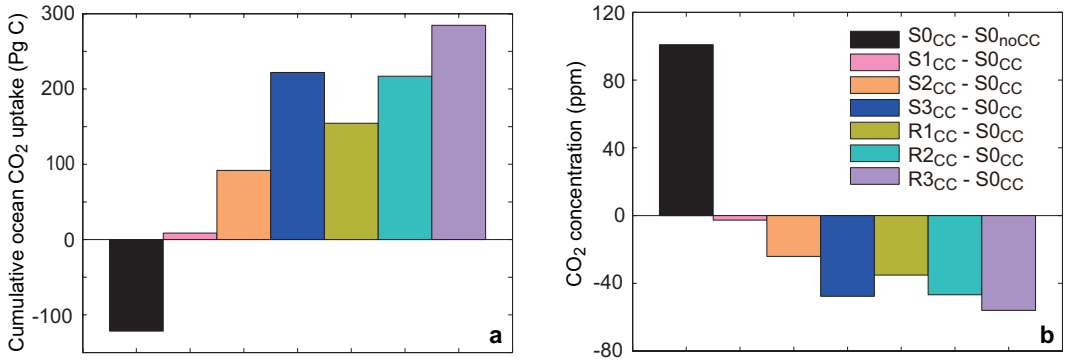

Figure 7. Simulated effects of different CO_2-calcification feedback parameterization schemes (colored bars) compared with the effect of CO_2-induced warming (black bars) in year 3500 for (a) cumulative ocean CO_2 uptake, (b) atmospheric CO_2 concentration. The effect of CO_2-calcification feedback is represented by the difference between S1 (S2, S3, R1, R2, R3) simulation with the inclusion of CO_2-induced warming and the S0 simulation with the inclusion of CO_2-induced warming. The effect of CO_2-induced warming is represented by the difference between S0 simulation with the inclusion of CO_2-induced warming and the S0 simulation without it. Detailed configuration of different model versions is provided in Table 1.

a CO_2 decrease of 12 ppm due to CO_2-calcification feedback when atmospheric CO_2 reaches about 1400 ppm[23]; Gangstø *et al.*[24], by using both Michaelis-Menten type formula and linear relationship to link calcification and $CaCO_3$ saturation, showed that by year 2100, the CO_2-calcification feedback acts to reduce atmospheric CO_2 concentration by 1 to 11 ppm under a range of parameterization schemes and IPCC scenarios of RCP8.5 and RCP6.0. Although these studies, including our study here, are not directly comparable because of different CO_2 pathways used and different inherent model structures in ocean dynamics and biogeochemistry, at least part of

the difference is associated with different representations of CO_2-calcification feedback. Uncertainties in our model results here reflect uncertainties in modeled parameterization of CO_2-calcification feedback, which actually reflects uncertainties in our understanding of the calcification response to changing ocean chemistry. The reported response of the $CaCO_3$ production rate to ocean acidification varies dramatically between experiments using different species of calcifying groups or manipulation methods[20,26]. Therefore, modeling simulations based on different results of experimental studies would result in different estimates of the effect of CO_2-calcification feedback. More coordinated experimental and observational studies on the $CaCO_3$ production response to ocean acidification are needed for a more reliable appraisal of the CO_2-calcification feedback.

In this study, we have investigated the response of calcification to acidification and its feedback to the ocean carbon cycle. Other processes relevant to $CaCO_3$ cycle that are not included in this study could also have important effect on the ocean carbon cycle. For example, inclusion of the dependence of $CaCO_3$ dissolution rate on $CaCO_3$ saturation state would further alter the ocean carbon cycle[19,27]. In addition, the ballast effect, i.e., the link between the fluxes of particulate organic carbon (POC) and particulate inorganic carbon (PIC) to the abyssal ocean[28,29], is not included in the model. It is possible that reduced $CaCO_3$ production could result in a decrease in PIC export rate, which consequently lowers POC export rate. This reduced vertical transport of POC would weaken the oceanic carbon pump and decrease the capacity for the global ocean to absorb atmospheric CO_2, acting as a positive feedback to atmospheric CO_2[22,30]. The feedback from the ballast effect could partly counteract the CO_2-calcification feedback, which merits further study.

This study demonstrates the potential important effect of CO_2-calcification feedback on the ocean carbon cycle and atmospheric CO_2 on the timescale from centuries to millennia. Further experimental and modeling studies are needed to acquire a better understanding of the CO_2-calcification feedback, which is crucial for a reliable projection of future atmospheric CO_2 concentrations and climate change.

Methods

Model description. An Earth system model of intermediate complexity, UVic ESCM (the University of Victoria Earth System Climate Model) version 2.9[31], was used for this study. UVic consists of a 3D ocean general circulation model (Modular Ocean Model 2 or MOM2) with a resolution of 1.8° latitude by 3.6° longitude and 19 vertical layers in the ocean. The ocean component is coupled to a vertically integrated energy-moisture balance atmospheric model and a thermodynamic/dynamic sea ice model[32]. The land carbon cycle component is represented by a dynamic vegetation model (the Hadley Center model TRIFFID) and a land surface model (the Met Office surface exchange scheme or MOSES)[33]. The ocean carbon cycle is represented by an inorganic carbon cycle model following the protocol of the Ocean Carbon-Cycle Model Intercomparison Project (OCMIP)[34], and a nutrient-phytoplankton-zooplankton-detritus (NPZD) marine ecosystem model[31]. The ocean carbon cycle model also comprises a sediment component that calculates $CaCO_3$ concentration from $CaCO_3$ dissolution and burial rates[35,36].

The $CaCO_3$ production in the model is calculated as

$$\mathrm{Pr}(\mathrm{CaCO_3}) = ((1-\gamma_1)\mathrm{G}(\mathrm{P_O})\mathrm{Z} + \mu_\mathrm{P}\mathrm{P_O^2} + \mu_\mathrm{Z}\mathrm{Z^2})\mathrm{R}^{\mathrm{CaCO_3/POC}}\mathrm{R_{C:N}} \quad (2)$$

where $\mathrm{Pr}(\mathrm{CaCO_3})$ represents $CaCO_3$ production, $(1-\gamma_1)\mathrm{G}(\mathrm{P_O})\mathrm{Z}$ denotes the zooplankton (Z) grazing of phytoplankton ($\mathrm{P_O}$), $\mu_\mathrm{P}\mathrm{P_O^2}$ represents the mortality of phytoplankton, $\mu_\mathrm{Z}\mathrm{Z^2}$ denotes the mortality of zooplankton, $\mathrm{R}^{\mathrm{CaCO_3/POC}}$ represents the ratio of $CaCO_3$ production to the production of particulate organic carbon, and $\mathrm{R}_{C:N}$ is the carbon to nitrogen Redfield ratio[31].

Parameterization of $CaCO_3$ production. In the original model, $CaCO_3$: POC production ratio $\mathrm{R}^{\mathrm{CaCO_3/POC}}$ in equation (2) is fixed at a constant value of 0.018. In this study, two types of parameterization functions of $\mathrm{R}^{\mathrm{CaCO_3/POC}}$ that link $CaCO_3$ production with saturation state of calcite (Ω_C) are introduced into the UVic model.

The first type of parameterization follows the Michaelis-Menten function based on Pinsonneault *et al.*[37]:

$$\mathrm{R}^{\mathrm{CaCO_3/POC}} = \mathrm{R}_{\mathrm{max}}^{\mathrm{CaCO_3/POC}}\left(\frac{(\Omega_\mathrm{C}-1)}{\mathrm{K_{max}} + (\Omega_\mathrm{C}-1)}\right) \quad (3)$$

Where $\mathrm{R}_{\mathrm{max}}^{\mathrm{CaCO_3/POC}}$ denotes the specified maximum value of $\mathrm{R}^{\mathrm{CaCO_3/POC}}$ (the $CaCO_3$: POC production ratio), and K_{max} is a half-saturation constant[37,38]. Different model versions based on this parameterization are denoted as "series S" (Table 1). In series S, the values of K_{max} are selected to be 0.07, 1.5 and 20, which covers the range of $\mathrm{K_{max}}$ values used by Pinsonneault *et al.*[37]. For each $\mathrm{K_{max}}$, we calculate the corresponding value of $\mathrm{R}_{\mathrm{max}}^{\mathrm{CaCO_3/POC}}$ by using the modeled preindustrial global mean sea surface calcite saturation state (Ω_C) of 5.2 to ensure that the preindustrial surface mean $CaCO_3$: POC production ratio in each model version has the same value of 0.018, i.e., the fixed constant used in the original model.

The second type of parameterization follows the thermodynamically-based function based on Ridgwell *et al.*[21,39]:

$$\mathrm{R}^{\mathrm{CaCO_3/POC}} = \mathrm{R}_0^{\mathrm{CaCO_3/POC}}(\Omega_\mathrm{C}-1)^\eta \quad (4)$$

Where $\mathrm{R}_0^{\mathrm{CaCO_3/POC}}$ represents a spatially-uniform constant and $(\Omega_\mathrm{C}-1)^\eta$ is a thermodynamically-based modifier with the power parameter η[21,39]. Different model versions based on this parameterization are denoted as "series

Michaelis-Menten Function: $R^{CaCO_3/POC} = R_{max}^{CaCO_3/POC}\left(\frac{(\Omega_C - 1)}{K_{max} + (\Omega_C - 1)}\right)$				
Model Version	K_{max}	$R_{max}^{CaCO_3/POC}$	$R^{CaCO_3/POC}$ at Preindustrial Surface Ω_C	Preindustrial Surface Ω_C
S1	0.07	0.0183	0.0180	5.2
S2	1.5	0.0244	0.0180	5.2
S3	20	0.1037	0.0180	5.2
Thermodynamically-based Function: $R^{CaCO_3/POC} = R_0^{CaCO_3/POC}(\Omega_C - 1)^{\eta}$				
Model Version	η	$R_0^{CaCO_3/POC}$	$R^{CaCO_3/POC}$ at Preindustrial Surface Ω_C	Preindustrial Surface Ω_C
R1	0.53	0.0084	0.0180	5.2
R2	0.81	0.0056	0.0180	5.2
R3	1.09	0.0038	0.0180	5.2
Control Simulation				
S0	—	—	0.0180	5.2

Table 1. Summary of configurations of different model versions with different parameterizations of the dependence of calcification rate on saturation state of $CaCO_3$.

R" (Table 1). In series R, we set the values of η to be 0.53, 0.81, and 1.09, which covers the range of η values used by Ridgwell *et al.*[21], and for each η we obtain the value of $R_0^{CaCO_3/POC}$ in the same way as $R_{max}^{CaCO_3/POC}$ in series S.

All together, we have a set of model versions with different parameterizations of $R^{CaCO_3/POC}$ (S1 to S3 and R1 to R3 in Table 1). In addition, we have the original model configuration with fixed $R^{CaCO_3/POC}$ (S0 in Table 1). For each parameterization, the dependence of $CaCO_3$: POC production ratio on Ω_C are presented in Fig. 1.

Simulation experiments. All of the model versions mentioned above are integrated for 10,000 model years with fixed preindustrial atmospheric CO_2 concentration of 280 ppm to reach a quasi-equilibrium preindustrial state of global climate and carbon cycle. Using the preindustrial climate state as initial condition for the nominal year of 1800, two sets of 1700-year transient simulations are performed (from year 1800 to 3500). The first set of simulation includes the feedback from CO_2-induced warming on the ocean carbon cycle, whereas the second set of simulation does not include the radiative effect of increasing CO_2 on global climate. Each set of experiments includes seven simulations, corresponding to the seven model versions listed in Table 1. All these 14 simulations are integrated under the IPCC CO_2 emission scenario SRES A2 ("business-as-usual") until year 2100. After year 2100, emissions are set to zero. During this spinup stage, at each time step continental weathering $CaCO_3$ flux via river discharge is set equal to the model-simulated accumulation flux of $CaCO_3$ from open ocean to deep-sea sediment. For transient simulations, weathering flux is held fixed at the rate that is diagnosed from the spinup run, whereas $CaCO_3$ accumulation flux is allowed to evolve freely.

References

1. Stocker, T. F. *et al.* In *Climate Change* 2013: The Physical Science Basis. Contribution of Working Group I to the Fifth Assessment Report of the Intergovernmental Panel on Climate Change (Cambridge University Press, Cambridge, United Kingdom and New York, NY, USA, 2013).
2. Le Quéré, C. *et al.* The global carbon budget 1959–2011. *Earth System Science Data Discussions* **5** (**2**), 1107–1157 (2012).
3. Caldeira, K. & Wickett, M. E. Anthropogenic carbon and ocean pH. *Nature* **425** (**6956**), 365 (2003).
4. Joos, F., Plattner, G. K., Stocker, T. F., Marchal, O. & Schmittner, A. Global warming and marine carbon cycle feedbacks an future atmospheric CO_2. *Science* **284** (**5413**), 464–467 (1999).
5. Plattner, G. K., Joos, F., Stocker, T. F. & Marchal, O. Feedback mechanisms and sensitivities of ocean carbon uptake under global warming. *Tellus B* **53** (**5**), 564–592 (2001).
6. Wohlers, J. *et al.* Changes in biogenic carbon flow in response to sea surface warming. *P Natl Acad Sci USA* **106** (**17**), 7067–7072 (2009).
7. Engel, A. Direct relationship between CO_2 uptake and transparent exopolymer particles production in natural phytoplankton. *J Plankton Res* **24** (**1**), 49–53 (2002).
8. Engel, A., Thoms, S., Riebesell, U., Rochelle-Newall, E. & Zondervan, I. Polysaccharide aggregation as a potential sink of marine dissolved organic carbon. *Nature* **428** (**6986**), 929–932 (2004).
9. Schartau, M. *et al.* Modelling carbon overconsumption and the formation of extracellular particulate organic carbon. *Biogeosciences* **4** (**4**), 433–454 (2007).
10. Feely, R. A. *et al.* Impact of anthropogenic CO_2 on the $CaCO_3$ system in the oceans. *Science* **305** (**5682**), 362–366 (2004).
11. Langdon, C. *et al.* Effect of calcium carbonate saturation state on the calcification rate of an experimental coral reef. *Global Biogeochem Cy* **14** (**2**), 639 (2000).
12. Gattuso, J. P., Frankignoulle, M., Bourge, I., Romaine, S. & Buddemeier, R. W. Effect of calcium carbonate saturation of seawater on coral calcification. *Global Planet Change* **18** (**1**), 37–46 (1998).
13. Zondervan, I., Zeebe, R. E., Rost, B. & Riebesell, U. Decreasing marine biogenic calcification: A negative feedback on rising atmospheric pCO(2). *Global Biogeochem Cy* **15** (**2**), 507–516 (2001).
14. Riebesell, U. *et al.* Reduced calcification of marine plankton in response to increased atmospheric CO_2. *Nature* **407** (**6802**), 364 (2000).
15. Barker, S. Foraminiferal Calcification Response to Glacial-Interglacial Changes in Atmospheric CO_2. *Science* **297** (**5582**), 833–836 (2002).
16. Kleypas, J. A. *et al.* Impacts of Ocean Acidification on Coral Reefs and Other Marine Calcifiers: A Guide for Future Research (NSF, NOAA, USGS, 2005).

17. Lombard, F., Da Rocha, R. E., Bijma, J. & Gattuso, J. P. Effect of carbonate ion concentration and irradiance on calcification in planktonic foraminifera. *Biogeosciences* **7** (**1**), 247–255 (2010).
18. Iglesias-Rodriguez, M. D. *et al.* Phytoplankton calcification in a high-CO_2 world. *Science* **320** (**5874**), 336–340 (2008).
19. Sarmiento, J. L. & Gruber, N. *Ocean Biogeochemical Dynamics*. (Princeton University Press, Princeton and Oxford, 2006).
20. Ridgwell, A. *et al.* From laboratory manipulations to Earth system models: scaling calcification impacts of ocean acidification. *Biogeosciences* **6** (**11**), 2611–2623 (2009).
21. Ridgwell, A., Zondervan, I., Hargreaves, J. C., Bijma, J. & Lenton, T. M. Assessing the potential long-term increase of oceanic fossil fuel CO_2 uptake due to CO_2-calcification feedback. *Biogeosciences* **4** (**4**), 481–492 (2007).
22. Hofmann, M. & Schellnhuber, H. J. Oceanic acidification affects marine carbon pump and triggers extended marine oxygen holes. *Proc Natl Acad Sci USA* **106** (**9**), 3017–3022 (2009).
23. Heinze, C. Simulating oceanic $CaCO_3$ export production in the greenhouse. *Geophys Res Lett* **31** (**16**) (2004).
24. Gangstø, R., Joos, F. & Gehlen, M. Sensitivity of pelagic calcification to ocean acidification. *Biogeosciences* **8** (**2**), 433–458 (2011).
25. Key, R. M. *et al.* A global ocean carbon climatology: Results from Global Data Analysis Project (GLODAP). *Global Biogeochem Cy* **18** (**4**) (2004).
26. Fielding, S. R. Predicting coccolithophore rain ratio responses to calcite saturation state. *Marine Ecology Progress Series* **500,** 57–65 (2014).
27. Ilyina, T. & Zeebe, R. E. Detection and projection of carbonate dissolution in the water column and deep-sea sediments due to ocean acidification. *Geophys Res Lett* **39** (**6**) (2012).
28. Armstrong, R. A., Lee, C., Hedges, J. I., Honjo, S. & Wakeham, S. G. A new, mechanistic model for organic carbon fluxes in the ocean based on the quantitative association of POC with ballast minerals. *Deep-Sea Res Pt Ii* **49** (**1–3**), 219–236 (2002).
29. Klaas, C. & Archer, D. E. Association of sinking organic matter with various types of mineral ballast in the deep sea: Implications for the rain ratio. *Global Biogeochem Cy* **16** (**4**), 61–63 (2002).
30. Gehlen, M. *et al.* Reconciling surface ocean productivity, export fluxes and sediment composition in a global biogeochemical ocean model. *Biogeosciences* **3** (**4**), 521–537 (2006).
31. Schmittner, A., Oschlies, A., Matthews, H. D. & Galbraith, E. D. Future changes in climate, ocean circulation, ecosystems, and biogeochemical cycling simulated for a business-as-usual CO_2. *Global Biogeochem Cy* **22,** GB1013, doi: 10.1029/2007GB002953. (2008).
32. Weaver, A. J. *et al.* The UVic Earth System Climate Model: Model description, climatology, and applications to past, present and future climates. *Atmos Ocean* **39** (**4**), 361–428 (2001).
33. Meissner, K. J., Weaver, A. J., Matthews, H. D. & Cox, P. M. The role of land surface dynamics in glacial inception: a study with the UVic Earth System Model. *Clim Dynam* **21** (**7–8**), 515–537 (2003).
34. Orr, J. C., Najjar, R., Sabine, C. L. & Joos, F. in *Internal OCMIP Report* (LSCE/CEA, Gifsur-Yvette, Saclay, France, 1999).
35. Archer, D. Modeling the calcite lysocline. *Journal of Geophysical Research-Oceans* **96** (**C9**), 17037–17050 (1991).
36. Archer, D. A data-driven model of the global calcite lysocline. *Global Biogeochem Cy* **10** (**3**), 511 (1996).
37. Pinsonneault, A. J., Matthews, H. D., Galbraith, E. D. & Schmittner, A. Calcium carbonate production response to future ocean warming and acidification. *Biogeosciences* **9** (**6**), 2351–2364 (2012).
38. Gehlen, M. *et al.* The fate of pelagic $CaCO_3$ production in a high CO_2 ocean: a model study. *Biogeosciences* **4** (**4**), 505–519 (2007).
39. Ridgwell, A. *et al.* Marine geochemical data assimilation in an efficient Earth System Model of global biogeochemical cycling. *Biogeosciences* **4** (**1**), 87–104 (2007).

Acknowledgements

This work is supported by National Natural Science Foundation of China (41276073; 41422503); National Key Basic Research Program of China (2015CB953601), the Fundamental Research Funds for the Central Universities (2015XZZX004-05); Zhejiang University K. P. Chao's High Technology Development Foundation.

Author Contributions

L.C. and Z.H. designed the research; L.C. and Z.H. performed model simulations and analysis; Both Z.H. and L.C. contributed to the writing of the paper.

Additional Information

Supplementary information accompanies this paper at http://www.nature.com/srep

Competing financial interests: The authors declare no competing financial interests.

How to cite this article: Zhang, H. and Cao, L. Simulated effect of calcification feedback on atmospheric CO_2 and ocean acidification. *Sci. Rep.* **6**, 20284; doi: 10.1038/srep20284 (2016).